Model for the linear electro-optic reflectance-difference spectrum of GaAs(001) around E_1 and $E_1+\Delta_1$

A. Lastras-Martínez
Instituto de Investigación en Comunicación Optica, Universidad Autónoma de San Luis Potosí, Alvaro Obregón 64, San Luis Potosí, S.L.P., Mexico

R. E. Balderas-Navarro
Facultad de Ciencias, Universidad Autónoma de San Luis Potosí, Alvaro Obregón 64, San Luis Potosí, S.L.P., Mexico

L. F. Lastras-Martínez and M. A. Vidal
Instituto de Investigación en Comunicación Optica, Universidad Autónoma de San Luis Potosí, Alvaro Obregón 64, San Luis Potosí, S.L.P., Mexico

(Received 23 September 1998)

We developed a model to describe the linear electro-optic (LEO) component of the reflectance-difference (RD) spectrum of zinc-blende semiconductors for energies around the E_1 and $E_1+\Delta_1$ critical points. The model is based on a piezoelectric effect due to the semiconductor surface electric field and predicts a LEO line shape given by the superposition of two terms, a first one proportional to the energy derivative of the reflectance spectrum and a second one associated with the undifferentiated reflectance spectrum. We compared the predictions of the model to experimental LEO line shapes for molecular-beam epitaxy GaAs(001) layers doped with 1.4×10^{16} cm^3 Si donors and found an excellent agreement. The results reported in this paper help develop the LEO RD spectroscopy as a characterization tool for zinc-blende semiconductors. [S0163-1829(99)02811-8]

I. INTRODUCTION

There is a growing interest in the use of reflectance-difference (RD) spectroscopy for the characterization of the surface electric field (SEF) in zinc-blende semiconductors. RD spectroscopy measures the difference in reflectance for two mutually orthogonal light polarizations and thus provides information on the breakdown of the zinc-blende cubic symmetry occurring at the semiconductor surface.[1] It is known that the RD spectrum of a number of zinc-blende (001) crystals show a linear electro-optic (LEO) component around the E_1 and $E_1+\Delta_1$ transitions, associated to the breakdown of the cubic symmetry by the semiconductor SEF.[2,3] The amplitude of this component depends linearly on the SEF strength and its sign on the sense of the SEF.[2–4] Information on, both, SEF strength and sense can be thus obtained from the LEO spectrum. RD measurements of LEO spectra around E_1 and $E_1+\Delta_1$ have been used for the *ex situ* characterization of the SEF in low-temperature grown MBE GaAs,[5,6] as well as for the contactless characterization of the impurity concentration in MBE ZnSe,[7,8] and for the characterization of the interface field in InP-$In_{0.53}Ga_{0.47}As$ heterojunctions.[9] Further applications of LEO-RD spectroscopy include the *in situ* determination of the impurity level of GaAs grown by MOCVD,[10] the characterization of the GaAs surface passivation[11] and the characterization of Si δ-doping in GaAs(001).[12]

Nevertheless, the application of the LEO spectroscopy to the characterization of the SEF in zincblende semiconductors has been limited because of the lack of a model to describe the LEO line shape around E_1 and $E_1+\Delta_1$. We note that such model is essential not only for applications were the LEO effect is directly involved, but also in those applications where it is necessary to subtract out the LEO component from the measured RD line shape, such as in RD studies of surface reconstruction during epitaxial growth.[13]

The LEO RD line shape for GaAs(100) shows contributions of opposite signs for the E_1 and $E_1+\Delta_1$ critical points. Very recently, Chen and Yang[14] have reported on a model for the LEO line shape around the E_1 and $E_1+\Delta_1$ transitions, based on a SEF piezoelectric effect. Such model predicts contributions of opposite signs for the E_1 and $E_1+\Delta_1$ critical points, but shows only a moderate agreement with the experimental LEO line shape.

In this paper we report on a model for the LEO line shape around E_1 and $E_1+\Delta_1$ which shows a remarkable agreement with the experimental spectrum of a GaAs(001) crystal. It is shown that the LEO line shape is obtained from the superposition of two components of comparable amplitude, a first one proportional to the energy-derivative of the reflectance spectrum R, and a second one associated to R. To allow for a comparison of the theoretical line shape model with experiment, we have measured a LEO line shape around E_1 and $E_1+\Delta_1$ for a GaAs MBE epitaxial layer doped with 1.4×10^{16} cm^3 Si donors. Care have been taken in order to obtain a LEO reflectance spectrum free from any component other than that of LEO origin. As pointed out before, we found an excellent agreement between theory and experiment.

The paper is organized as follows. In Sec. II we give experimental details on the measurement of the LEO spectrum. In Sec. III we develop the model for the LEO line shape. In Sec. IV we compare the experimental LEO spec-

trum to the theoretical line shape and finally in Sec. V we give the conclusions to the paper.

II. EXPERIMENTAL

The LEO reflectance spectrum analyzed in this paper was obtained by subtracting two photoreflectance (PR) spectra for a (001)-oriented GaAs crystal. One of the spectra was taken with unpolarized light and the other with light polarized along $[1\bar{1}0]$. Obtaining the LEO line shape from PR measurements rather than from RD measurements allows us to suppress in a straightforward way spectral components not of LEO origin, which are known to be very prominent in RD spectra for energies around the E_1 and $E_1+\Delta_1$ transitions.[2,3] As it is shown elsewhere,[2,15,16] the polarized-light PR spectrum of (001) zinc-blende semiconductors comprises, both, linear and quadratic components and may be written as

$$\frac{\Delta R}{R}=2\lambda\mu P_{123}F+Q_{12}F^2, \tag{1}$$

where F is the strength of the modulated surface electric field that is assumed to be along [001], p_{123} and Q_{12} are components of the tensors (third and fourth-rank, respectively) describing linear and quadratic electro-optic effects, respectively, and λ and μ are the direction cosines of the polarization vector of the incident light. We note in Eq. (1) that, while the linear line shape is polarization-dependent, the quadratic spectrum is isotropic. Thus, the unpolarized light PR spectra should comprise only the quadratic component, since the linear component averages out to zero. In this way, by subtracting the unpolarized light spectrum from the polarized-light spectrum we obtain the LEO spectrum.

The sample employed for the PR measurements was a 1 μm thick Si-doped GaAs epitaxial layer grown by MBE on a semi-insulating GaAs substrate. The *n*-type doping level of the GaAs epilayer was of $1.4\times10^{16}\,\mathrm{cm}^3$, as determined from Hall effect measurements. The PR experiments were carried out in a spectrometer employing a Xe lamp as a light source and a 0.25 m monochromator with a grating optimized at $\lambda=0.5\,\mu$m. A silicon photodiode was used to detect the light reflected by the sample. A mechanically chopped 10 mWatt He-Ne laser was used for the modulation of the sample SEF. The corresponding changes in sample reflectivity were measured by phase-sensitive techniques. Furthermore, to allow for both polarized and unpolarized PR measurements, a Rochon prism and a photoelastic modulator were placed in between the monochromator and the sample, as shown schematically in Fig. 1. Polarized light measurements were carried out by turning the photoelastic modulator off. Unpolarized light spectra were taken with the photoelastic modulator turned on, by taking advantage of the large difference between the laser chopping frequency (150 Hz) and the polarization modulation frequency (100 kHz). The maximum phase retardation of the photoelastic modulator was adjusted to $\lambda/2$ in the whole wavelength scanning range. Both polarized and unpolarized light data were obtained sequentially at each wavelength, before stepping the monochromator to next wavelength. To perform this operation the photoelastic modulator on/off switching operation was controlled by the spectrometer computer. This procedure eliminates errors due to monochromator wavelength backlash when taking the polarized-unpolarized PR difference spectra. Otherwise, such backlash could lead to a considerably error in the PR difference spectrum, due to the sharpness of the quadratic electro-optic PR line shape[17] as compared with the LEO line shape. Reflectance measurements were carried out in a Varian Cary-5 spectrophotometer.

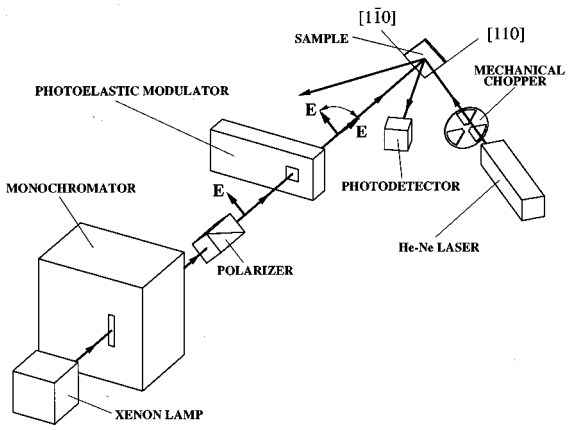

FIG. 1. Schematics of the PR spectrometer employed in this work.

III. LINE SHAPE MODEL

Let we consider the (001) surface of an *n*-type zinc-blende semiconductor with a surface electric **F** pointing along [001]. This electric field induces a piezo-electric strain near the semiconductor surface that reduces the semiconductor symmetry from cubic (T_d) to orthorhombic (C_{3v}). The nonzero strain components are given by[18]

$$e_{xy}=e_{yx}=d_{14}F, \tag{2}$$

where d_{14} is the piezo-electric modulus. Strain tensor (2) leads to a tensorial change $\Delta\tilde{\varepsilon}_{xy}=\Delta\tilde{\epsilon}_{yx}$ in the semiconductor complex dielectric function. We are interested in determining such a change for light normally incident on the (001) surface with polarization along $[1\bar{1}0]$, for energies around E_1 and $E_1+\Delta_1$. We note that $[1\bar{1}0]$ corresponds to one of the two directions of maximum change for $\Delta\tilde{\epsilon}_{xy}$.

E_1 and $E_1+\Delta_1$ interband transitions are known to originate from Λ symmetry points in the Brillouin zone.[19] In the unperturbed zincblende crystal there are 8 equivalent Λ points. It is not difficult to see from geometrical considerations that in the presence of the strain defined in Eq. (2) these 8 points are no longer equivalent but split apart into two sets of 4 equivalent points, a first set containing points along [111], $[\bar{1}\bar{1}1]$, $[1\bar{1}1]$ and $[\bar{1}1\bar{1}]$, and a second set containing points along $[\bar{1}\bar{1}1]$, $[\bar{1}1\bar{1}]$, $[1\bar{1}\bar{1}]$ and $[\bar{1}\bar{1}\bar{1}]$. In what follows we will label with subscript 111 the critical points in the first set and with $1\bar{1}\bar{1}$ those in the second set.

It can be shown (see Appendix A) that in the strained crystal the E_1 and $E_1+\Delta_1$ interband transition energies are shifted in energy by[20] (see Fig. 2)

$$\delta E=\pm\gamma(1+2B^2d'/d), \tag{3}$$

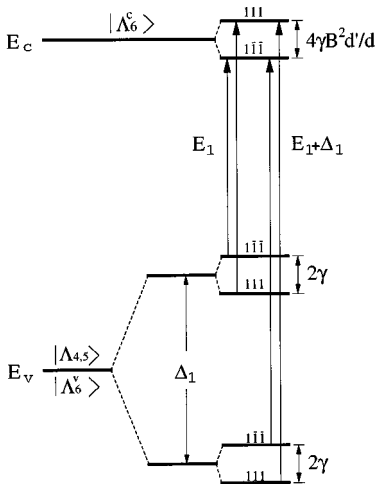

FIG. 2. Energy levels for Λ points in the presence of the piezoelectric strain given by Eq. (2).

where ± correspond, respectively, to critical points in the first and second sets defined above, d and d' are the deformation potentials of the valence band and the conduction band, respectively, $\gamma = d d_{14} F/\sqrt{3}$ and B is a parameter defined in Eq. (A3).

We will write the overall change in the complex dielectric function $\Delta\tilde{\varepsilon}_{xy}$ as

$$\Delta\tilde{\varepsilon}_{xy} = \Delta\tilde{\varepsilon}'_{xy} + \Delta\tilde{\varepsilon}''_{xy}, \tag{4}$$

where $\Delta\tilde{\varepsilon}'_{xy}$ and $\Delta\tilde{\varepsilon}''_{xy}$ correspond to the contributions associated to points E_1 and $E_1+\Delta_1$, respectively. By following the approach described elsewhere,[21] we can write for $\Delta\tilde{\varepsilon}'_{xy}$ (with an equivalent expression for $\Delta\tilde{\varepsilon}''_{xy}$)

$$\Delta\tilde{\varepsilon}'_{xy} = \frac{C}{E^2}[M_{111}J(E,E_0+\Delta E_0) + M_{1\bar{1}1\bar{1}}J(E,E_0-\Delta E_0) - M_0 J(E,E_0)], \tag{5}$$

where $\Delta E_0 = |\delta E|$, E_0 is the interband transition energy in the absence of perturbations, J the interband joint density of states, M_{111} and $M_{1\bar{1}1\bar{1}}$ are the squared interband transition matrix elements for the perturbed crystal, M_0 is the corresponding matrix element for the unperturbed crystal and C is a constant independent of energy.[21]

It can be shown (see Appendix A) that the squares of the interband transition matrix elements for light polarization along $[1\bar{1}0]$ are given by

$$M_{111} = \frac{3}{4}\left(1 \pm \frac{4\gamma}{\Delta_1}\right) M_0, \tag{6a}$$

$$M_{1\bar{1}1\bar{1}} = \frac{1}{4}\left(1 \pm \frac{4\gamma}{\Delta_1}\right) M_0, \tag{6b}$$

were signs ± correspond to transitions E_1 and $E_1+\Delta_1$, respectively. By taking into account that $\partial\tilde{\varepsilon}/\partial E = -\partial\tilde{\varepsilon}/\partial E_0$, from Eqs. (4)–(6) we obtain

$$\Delta\tilde{\varepsilon}_{xy} = -\frac{1}{2E^2}\frac{\partial[E^2(\tilde{\varepsilon}'+\tilde{\varepsilon}'')]}{\partial E}\Delta E_0 + \frac{4\gamma}{\Delta_1}(\tilde{\varepsilon}'-\tilde{\varepsilon}''), \tag{7}$$

where $\tilde{\varepsilon}'$ and $\tilde{\varepsilon}''$ stand, respectively, for the contribution of the E_1 and $E_1+\Delta_1$ critical points to the overall complex dielectric function $\tilde{\varepsilon}$.

By writing the LEO line shape as $\Delta R/R = \mathrm{Re}[(\alpha+\beta)\Delta\tilde{\varepsilon}]$, where α and β are Seraphin coefficients, Eq. (7) allows us to write

$$\frac{\Delta R}{R} = -\frac{1}{2E^2}\mathrm{Re}\left[(\alpha - i\beta)\frac{\partial(E^2\tilde{\varepsilon})}{\partial E}\right]\Delta E_0 + \frac{4\gamma}{\Delta_1}\mathrm{Re}[(\alpha - i\beta)(\tilde{\varepsilon}'-\tilde{\varepsilon}'')]. \tag{8}$$

Equation (8) shows that the $\Delta R/R$ line shape is given by the superposition of two terms, a first term proportional to the first-energy derivative of the sample reflectivity and a second term proportional to the difference in the dielectric functions associated to E_1 and $E_1+\Delta_1$. We note that the first term, analogous to that of first-derivative spectroscopies such as thermoreflectance,[22] leads to a relatively narrow line shape that is determined to a large extent by transitions around the resonance energies E_1 and $E_1+\Delta_1$. Such lineshape results relatively simple to model in terms of Lorenzian functions.[17] In contrast, a line shape proportional to $\tilde{\varepsilon}$ may include contributions from broader energy regions and therefore may prove to be more difficult to model. It turns out, moreover, that since the second term in the right-hand side of Eq. (8) is proportional to the difference in dielectric functions of two critical points relatively close in energy, it leads to a relatively narrow line shape. As it is shown in next section, this lineshape can be modeled in terms of Lorenzian functions. We should further note that Eq. (8) corresponds to the LEO spectrum that arises from taking the difference between the zero SEF reflectance and the reflectance with a SEF of strength F. Finally, we note that according to Eq. (1) the LEO spectrum as obtained from RD measurements would have an amplitude twice as large as that of Eq. (8).

IV. EXPERIMENTAL RESULTS AND DISCUSSION

Broken and solid lines in Fig. 3 show the PR spectra of our GaAs sample, for unpolarized light and for light polarized along $[1\bar{1}0]$, respectively. As discussed above, the LEO spectrum can be obtained by subtracting the broken line spectrum from the solid line spectrum. Dots in Fig. 4 show the linear PR lineshape obtained in this way. We note that this line shape is relatively narrow as predicted by Eq. (8). In fact, Eq. (8) predicts remarkably well the experimental lineshape of Fig. 4 as described in what follows.

We first note that since reflectance data are more readily available than dielectric function data for a specific sample, we will put the line shape given in Eq. (8) solely in terms of the reflectance spectrum. To do so, we note that in the energy interval of interest to us around E_1 and $E_1+\Delta_1$ we may write

$$\mathrm{Re}[(\alpha - i\beta)\tilde{\varepsilon}] = -R + f, \tag{9}$$

where f is a function that is weakly dependent on energy. Relation (9) may be readily validated by substitution of the

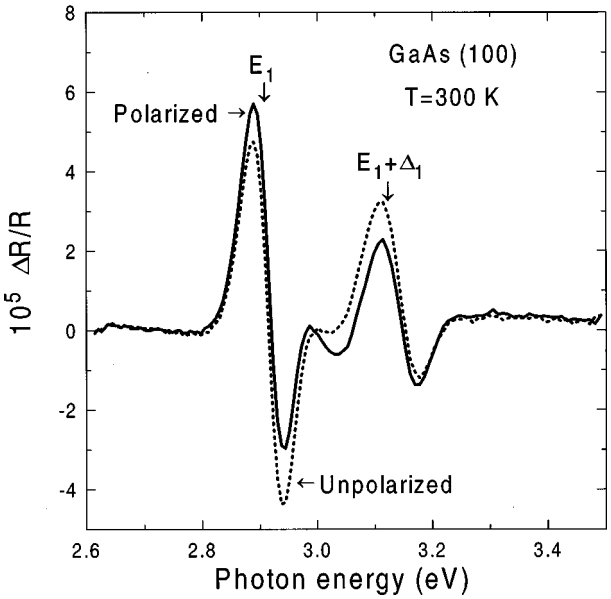

FIG. 3. PR spectra for a GaAs epitaxial layer doped with $1.4 \times 10^{16}\,\mathrm{cm}^3$ Si donors. Solid and broken lines correspond to polarized light along $[1\bar{1}0]$ and to unpolarized light, respectively.

experimental dielectric function data. By making use of Eqs. (8) and Eq. (9) we may write approximately for the LEO reflectance line shape

$$\frac{\Delta R}{R} = -\frac{1}{2R}\frac{\partial R}{\partial E}\Delta E_0 + \frac{4\gamma}{\Delta_1}(R' - R''), \tag{10}$$

where R' and R'' are Lorenzian line shapes representing the contributions to sample reflectivity of critical points E_1 and $E_1+\Delta_1$ respectively. R' and R'' are obtained by fitting the sample reflectance spectrum to $R'+R''$ in an energy interval

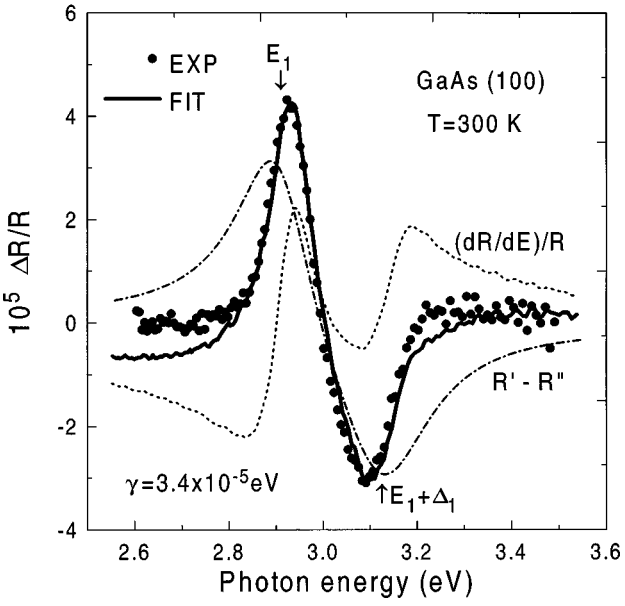

FIG. 4. Linear electro-optic reflectance line shapes. Dots correspond to experimental points while the solid line is the fitting to the theoretical model developed in this work. Dashed lines correspond to the two components of the solid line spectrum.

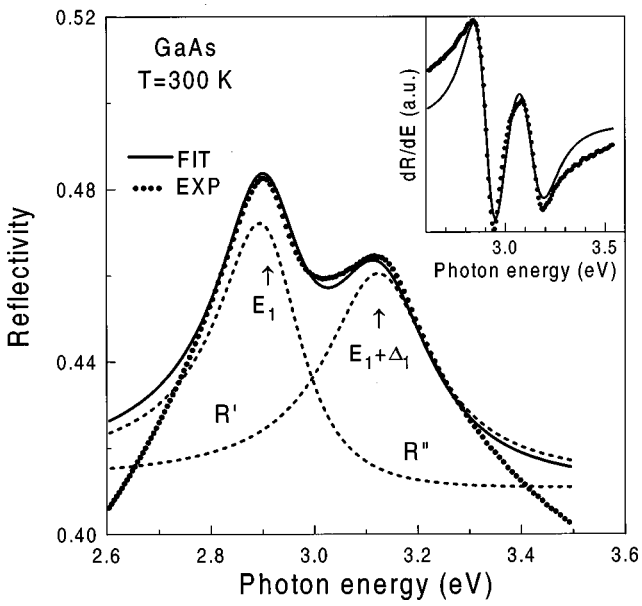

FIG. 5. Dotted line: experimental reflectance line shape for the GaAs sample studied in this work. Solid line: best fitting of the reflectance line shape around E_1 and $E_1+\Delta_1$ to the superposition of two Lorenzian line shapes, one centered at E_1 and the other at $E_1+\Delta_1$. Broken lines: individual Lorenzian line shapes of the solid line fitting. Inset: Energy derivative of the experimental reflectance spectrum (dots) and energy derivative of the best fitting line shape (solid line).

around E_1 and $E_1+\Delta_1$, as shown in Fig. 5. Lorenzian line shapes R' and R'' are centered at the E_1 and $E_1+\Delta_1$ energies, respectively. Dots in Fig. 5 give the experimental R spectrum while solid line represents the best fitting obtained. We note from the inset in Fig. 5 that the energy-derivative of this fitting reproduce quite well all the features of the energy-derivative reflectance spectrum. Broken lines correspond to lineshapes R' and R'' as indicated.

Solid line in Fig. 4 shows the fitting of Eq. (10) to the experimental LEO reflectance spectrum. Dashed lines show the two components of the overall LEO spectrum as indicated. For this fitting we have employed the values, $\Delta_1 = 0.21\,\mathrm{eV}$, $d = 5.4\,\mathrm{eV}$, $d' = 5.0\,\mathrm{eV}$ and $B = 0.56$.[20] As it can be seen, despite the fact that only one fitting parameter was employed (the spectrum amplitude) there is a remarkable agreement between the experimental line shape and Eq. (10), showing that the model developed in Sec. III is adequate to describe LEO reflectance lineshapes in zinc-blende semiconductors. As it can be seen from Fig. 4, these two components are of comparable amplitude, showing that both have to be taken into account to properly fit the experimental LEO line shape. Furthermore, Fig. 4 shows that the opposite sign of the E_1 and $E_1+\Delta_1$ critical point contributions arises to a large extent from the spectrum component proportional to $R'-R''$. Nevertheless, the observed energy positions of the maximum and minimum of the LEO spectrum, that appear shifted with respect to the critical point energies as pointed out before,[14] are a consequence of the superposition of, both, $R'-R''$ and $(dR/dE)/R$ line shapes. Furthermore, we can see that the LEO spectrum of Fig. 4 shows that the broadening of the positive peak around E_1 is smaller that of the negative peaks around $E_1+\Delta_1$. This feature is as well a

consequence of the fact that the LEO spectrum arises from the superposition of two line shapes with quite different optical structures.

From the fitting of Fig. 4 we obtain $\gamma = 3.4 \times 10^{-5}$ eV. By using this value along with the experimental value for the piezoelectric modulus of GaAs $d_{14} = 2.7 \times 10^{-10}$ cm/V,[23] we get $F \approx 4 \times 10^4$ V/cm for the average strength of the electric field that gives rise to the LEO effect. By assuming a surface potential of 1 V, the average surface field is estimated to be $\approx 5 \times 10^4$ V/cm, which is close to the strength of the field F.

V. CONCLUSIONS

We have developed a model to describe LEO line shapes in the RD spectrum of zinc-blende semiconductors. The model is based on a piezo-electric effect associated to the semiconductor SEF. We obtained a LEO line shape that is given by the superposition of two components, a first one proportional to the energy-derivative of the reflectance spectrum, and a second one associated to the undifferentiated reflectance spectrum. In order to make a comparison with experiment we have measured the LEO reflectance line shape for a GaAs(001) epitaxial layer doped with 1.4 $\times 10^{16}$ cm^3 Si donors. This line shape has been determined through PR measurements. We found a remarkable agreement between theory and experiment. The results reported in this paper help develop the LEO RD spectroscopy as a characterization tool for zinc-blende semiconductors, specifically for the characterization of surface electric fields.

ACKNOWLEDGMENTS

The authors are grateful to H. Navarro-Contreras for many helpful discussions and for his careful reading of the manuscript. This work was supported by the Consejo Nacional de Ciencia y Tecnología through Grants No. F219 and 0691P-E, and by the Organization of American States.

APPENDIX

The effect of piezoelectric strain on the valence band energy at Λ critical points may be determined through the Bir-Pikus Hamiltonian[20,24]

$$H_v = -3\gamma(L_x L_y + L_y L_x) + \frac{1}{2}\Delta_1 \mathbf{L}\cdot\mathbf{s}, \tag{A1}$$

where **L** and **s** are the angular momentum and spin operators, respectively, and γ is defined in main text. A similar Hamiltonian, with appropriate parameters, holds for the conduction band.

In the absence of, both, spin-orbit and piezoelectric interactions, the valence band wave functions E_1 and $E_1+\Delta_1$, for the critical point along [111], are given, respectively, by[20]

$$|\Lambda_{4,5}^{v}\rangle = \frac{1}{2}\left[X - Y + \frac{i}{\sqrt{3}}(X + Y - 2Z)\right]|\uparrow\rangle, \tag{A2a}$$

$$|\Lambda_{6}^{v}\rangle = \frac{1}{2}\left[X - Y - \frac{i}{\sqrt{3}}(X + Y - 2Z)\right]|\uparrow\rangle, \tag{A2b}$$

while the conduction band wave function is given by

$$|\Lambda_{6}^{c}\rangle = A|S\uparrow\rangle + \frac{B}{\sqrt{3}}(x + y + z)|\uparrow\rangle, \tag{A3}$$

where $A = -B = 0.56$ for GaAs.[20] Equivalent wave functions can be written for the $[1\bar{1}\bar{1}]$ critical point.

Perturbation Hamiltoninan (A1) removes the equivalence of the eight Λ points, ordering them in two sets of equivalent points, $\{[111],[\bar{1}\bar{1}\bar{1}],[1\bar{1}\bar{1}],[\bar{1}1\bar{1}]\}$ (set 1) and $\{[\bar{1}\bar{1}1],[\bar{1}1\bar{1}],[1\bar{1}1],[1\bar{1}\bar{1}]\}$ (set 2). The perturbed valence band wave functions are

$$|E_1\rangle = |\Lambda_{4,5}^{v}\rangle \pm \frac{2\gamma}{\Delta_1}|\Lambda_{6}^{v}\rangle, \tag{A4a}$$

$$|E_1 + \Delta_1\rangle = |\Lambda_{6}^{v}\rangle \mp \frac{2\gamma}{\Delta_1}|\Lambda_{4,5}^{v}\rangle, \tag{A4b}$$

where signs $\pm$ in Eq. (A4a) and $\mp$ in Eq. (A4b) apply to the first and to the second sets of critical points, respectively. Unperturbed wave functions in Eqs. (A4a) and (A4b) are those appropriate to the critical point set considered.

We obtain for the changes in interband transition energies

$$E_r^{1,2} = r\frac{1}{2}\Delta_1 + r\frac{4\gamma^2}{\Delta_1} \pm \gamma(1 + 2B^2 d'/d), \tag{A5}$$

where index $r = \pm 1$ stands for E_1 and $E_1+\Delta_1$ levels, respectively. We note that, since in our case $\gamma/\Delta_1 \ll 1$, we can neglect the second term in the right-hand side of Eq. (A5).

Finally, from Eq. (A3) and Eqs. (A4a) and (A4b) we obtain, for light polarization along $[1\bar{1}0]$, the interband transition matrix elements given by Eqs. (6a) and (6b) in the main text.

[1] D. E. Aspnes and A. A. Studna, Phys. Rev. Lett. **54**, 1956 (1985).

[2] S. E. Acosta-Ortíz and A. Lastras-Martínez, Phys. Rev. B **40**, 1426 (1989); in *International Conference on Modulation Spectroscopy*, edited by Fred H. Pollak, Manuel Cardona, and David E. Aspnes, Proc. SPIE Vol. No. 1286 (SPIE, Bellingham, WA, 1990), p. 31.

[3] S. E. Acosta-Ortiz and A. Lastras-Martínez, Solid State Commun. **64**, 809 (1987).

[4] Z. Yang, Y. H. Chen, and Yuqi Wong, Appl. Phys. Lett. **73**, 1520 (1998).

[5] Todd Holden, Fred H. Pollak, J. L. Freeouf, D. McInturff, J. L. Gray, M. Lundstrom, and J. M. Woodall, Appl. Phys. Lett. **70**, 1107 (1997).

[6] Y. H. Chen, Z. Yang, R. G. Li, and Y. Q. Wang, Phys. Rev. B **55**, R7379 (1997).

[7] H. H. Farrell, M. C. Tamargo, T. J. Gmitter, A. L. Weaver, and D.

E. Aspnes, J. Appl. Phys. **70**, 1033 (1991).
[8] Chen-Guo Jin, Tetsuji Yasuda, Kozo Kimura, Akihiro Ohtake, Li-Hsin Kuo, Tai-Hong Huang, Shiro Miwa, Takafumi Yao, and Kazunobu Tanaka, Jpn. J. Appl. Phys., Part 1 **36**, 6638 (1997).
[9] M. Leibovitch, P. Ram, L. Malikova, Fred. H. Pollak, J. L. Freeouf, L. Kronik, B. Mishori, Yoram Shapira, A. R. Clawson, and C. M. Hanson, J. Vac. Sci. Technol. B **14**, 3089 (1996).
[10] H. Tanaka, E. Colas, I. Kamiya, D. E. Aspnes, and R. Bhat, Appl. Phys. Lett. **59**, 3443 (1991).
[11] V. L. Berkovits, V. N. Bessolov, T. N. L'vova, E. V. Novikov, V. I. Safarov, R. V. Khasieva, and B. V. Tsarenkov, J. Appl. Phys. **70**, 3707 (1991).
[12] Z. Sobiesierski, D. I. Westwood, and M. Elliot, Phys. Rev. B **56**, 15 277 (1997).
[13] T. B. Joyce, T. Farrell, and B. R. Davidson, J. Cryst. Growth **188**, 211 (1998).
[14] Y. H. Cheng and Z. Yang, Appl. Phys. Lett. **73**, 1667 (1998).
[15] D. E. Aspnes and A. A. Studna, Phys. Rev. B **7**, 4605 (1973).
[16] R. Kyser and Victor Rhen, Solid State Commun. **8**, 1437 (1970).
[17] See, e.g., D. E. Aspnes, in *Handbook on Semiconductors*, edited by M. Balkanski (North-Holland, Amsterdam, 1980), Vol. 2, p. 121.
[18] See, e.g., J. F. Nye, *Physical Properties of Crystals* (Oxford University Press, Oxford, 1995), p. 115.
[19] See, e.g., Peter Y. Yu and M. Cardona, *Fundamentals of Semiconductors* (Springer-Verlag, Berlin, 1996), p. 256.
[20] F. H. Pollak and M. Cardona, Phys. Rev. **172**, 816 (1968).
[21] L. F. Lastras-Martínez and A. Lastras-Martínez, Phys. Rev. B **54**, 10 726 (1996).
[22] M. Cardona, in *Solid State Physics*, edited by F. Seitz, F. Turnbull, and H. Ehrenreich (Academic, New York, 1969), Suppl. 11.
[23] *Physics of Group IV Elements and III–V Compounds*, edited by O. Madelung, Landolt Börnstein, New Series, Vol. III/17a (Springer, Berlin, 1982), p. 241.
[24] G. L. Bir and G. E. Pikus, *Symmetry and Strain-Induced Effects in Semiconductors* (Wiley, New York, 1974), p. 295.